

ANISOTROPIC PRESSURE AND HYPERONS IN NEUTRON STARS

A. Sulaksono

*Departemen Fisika, FMIPA, Universitas Indonesia,
Depok, 16424, Indonesia*

Received (received date)

Revised (revised date)

We study the effects of anisotropic pressure on properties of the neutron stars with hyperons inside its core within the framework of extended relativistic mean field. It is found that the main effects of anisotropic pressure on neutron star matter is to increase the stiffness of the equation of state, which compensates for the softening of the EOS due to the hyperons. The maximum mass and redshift predictions of anisotropic neutron star with hyperonic core are quite compatible with the result of recent observational constraints if we use the parameter of anisotropic pressure model $h \leq 0.8^1$ and $\Lambda \leq -1.15.^2$ The radius of the corresponding neutron star at $M=1.4 M_\odot$ is more than 13 km, while the effect of anisotropic pressure on the minimum mass of neutron star is insignificant. Furthermore, due to the anisotropic pressure in the neutron star, the maximum mass limit of higher than $2.1 M_\odot$ cannot rule out the presence of hyperons in the neutron star core.

Keywords: Neutron star; hyperons; anisotropic pressure

PACS numbers:97.60.Jd;14.20.Jd;26.60.Kp

1. Introduction

The most accurate measurement in identifying the masses of neutron star (NS) is the number of pulsars in the bound binary systems (neutron-neutron and neutron-white dwarf systems). Based on a recent analysis on mass distribution of the number of pulsars with secure mass measurement, $M_G \sim 2.1 M_\odot$ can be considered as an established value of lower bound on maximum mass (M_{max}) for NS.³ Therefore, the existence of more massive NSs is, in principle, possible. The NS maximum mass establishment comes from the result of two accurate NS mass measurements. The mass $1.97 \pm 0.04 M_\odot$ of pulsar J1614-2230 is measured from the Shapiro delay⁴ and the mass $2.01 \pm 0.04 M_\odot$ ⁵ of pulsar J0348+0432 is measured from the gravitational redshift optical lines of its white dwarf companion. In addition, there are evidences that some black widow pulsars might have higher masses. For example, pulsar B1957+20 reportedly has a mass of $M_G = 2.4 \pm 0.12 M_\odot$,⁶ and even gamma-ray black widow pulsar J1311-3430⁷ has higher mass than B1957+20 but with less accuracy. This NS maximum mass limit poses a tight constraint on

the equation of state (EOS) of dense matter in the NS core. However, we point out that over the time, with new planned observatories and technology advancement in astrometry, it is not impossible to have accurately measured pulsar mass of higher than $2.1 M_{\odot}$ in the future.^{8,10,11} For the latest review on neutron star masses and their implications we refer the reader to Refs. 8-11. It is also worthy to note that actually accurate measurements of the NS radii would also strongly constrain the properties of the matter in NS core. Unfortunately, the analysis methods used to extract NS radii from observational data still have high uncertainty and mostly they come from systematics.⁸ Furthermore, the limits of recent observational radii from different sources or even from the same source are often in contradictory one to another.¹²⁻¹⁹

The observational constraint on the lower bound of the maximum NS mass of $2.1 M_{\odot}$ can be readily fulfilled by most models if NS core contains only nucleons and leptons. For examples IUFSU parameter set²⁰ yields $M_{\max} = 1.94 M_{\odot}$ and BSP parameter set²¹ yields $M_{\max} = 2.02 M_{\odot}$. On the other hand, the presence of only nucleons and leptons in NS core is physically not too realistic. In general the nuclear models that are compatible with the experimental data on hyper-nuclei predict the existence of hyperons in matter at the density of exceeding 2-3 times nuclear saturation density ($\rho_0 = 0.16 \text{ fm}^{-3}$).²² Furthermore, the presence of exotic particles such as hyperons in NS core has important impact on NS cooling.²³ The hyperonization of matters tends to soften the EOS of NS core as the energetic nucleons are replaced by slow moving hyperons. Consequently, the predicted maximum mass of NS with hyperons in its core is always smaller than that of NS without hyperons.^{23,24} We note that the Brueckner-Hartree-Fock (BHF) model^{25,26} yields $M_{\max} \sim 1.3-1.4 M_{\odot}$ if hyperons are included in the EOS of NS core. It is reported by the authors of Ref. 27 that 3-body force also cannot help much to increase the predicted NS maximum mass, but it is shown recently by the authors of Ref. 28 that 3-body forces can increase the maximum mass significantly. In relativistic mean field (RMF) models, the situation is quite similar, $M_{\max} \sim 2.1 M_{\odot}$ can be reached only by adjusting the model parameters in the hyperon sector or modifying nonlinear in the strange sector or introducing hypothetical weakly interacting light boson (WILB).²⁹⁻³³ The puzzle that whether or not the hyperons are present in the NS core has triggered the theoreticians to revisit the NS models (see Refs. 34-40 for details). The anticipation of accurate measurement of NS with the mass of greater than $2.1 M_{\odot}$ possible in the future, the parameters and model adjustments in the framework of RMF models with acceptable nuclear EOS at low and moderate densities may no longer be the best way to handle maximum mass.

Usually one assumes that the pressure in the NS is isotropic. But, there are arguments (see Ref. 41 and the references therein) that the matter pressure of NS may be slightly different among different directions (anisotropic). This effect can be caused by many interrelated factors such as the presence of strong magnetic and electric fields, boson condensations, different kinds of phase transition, the ex-

istence of solid core or super fluidity, etc. This is also supported by Herrera and Santos stating that formally, the mixture of two fluids is mathematically equivalent to an anisotropic fluid (see Ref. 41 and the references therein). Furthermore, it has been shown that at high density the nuclear matter pressure can also be anisotropic (see for example Refs. 42-43). Since the pioneer work of Bowers and Liang,⁴⁴ there have been many works devoted to studies of anisotropic spherical symmetric configurations. Recent studies on the properties of anisotropic star can be found for examples in Refs.1-2 while studies for other anisotropic configurations can be found in Refs. 45,47-49. These studies reveal that anisotropy may have effects on maximum equilibrium mass and gravitational redshift.

In this work, we argue that “hyperonization puzzle” can be solved by considering that the pressure in NS matter may be anisotropic. We study the NS mass, radius and the gravitational redshift of anisotropic NS within the framework of the extended version of relativistic mean field (ERMF) model.^{21,50,51}

The paper is organized as follows. Sec. 2, describes the brief outline of NS EOS. Sec. 3, discussion on anisotropic pressure configuration. Section 4 is devoted to discussion of the results. Finally Sec. 5 is conclusion.

2. Equation of State

In general, NS has three parts with different compositions and density ranges i.e., outer crust, inner crust and the core. In this work, the crust EOS by Miyatsu *et al.*³⁹ is taken to describe NS crusts. The core is assumed to be composed of baryons and leptons and the corresponding EOS is calculated by using the ERMF model.

The ERMF model includes contribution from the standard RMF nonlinear self-interaction for σ and ω mesons as well as additional cross interaction terms for σ , ω and ρ mesons. The detail of this model and the EOS derivation based on this model are well documented.^{50,51} In the ERMF model, baryons interact through exchanges of σ , ω , ρ and ϕ mesons, while the baryons involved are nucleons ($N=p$ and n) and hyperons ($H=\Lambda$, Σ and Ξ). Thus the total Lagrangian density, including leptons ($l=e$ and μ) for calculating the EOS of NS core can be written as³⁰

$$\mathcal{L} = \mathcal{L}_B^{\text{free}} + \mathcal{L}_M^{\text{free}} + \mathcal{L}_{BM}^{\text{lin}} + \mathcal{L}^{\text{nonlin}} + \mathcal{L}_l^{\text{free}}, \quad (1)$$

where the free baryons Lagrangian density is,

$$\mathcal{L}_B^{\text{free}} = \sum_{B=N,\Lambda,\Sigma,\Xi} \bar{\Psi}_B [i\gamma^\mu \partial_\mu - M_B] \Psi_B, \quad (2)$$

Here, Ψ_B is baryons field and the sum is taken from N , Λ , Σ , and Ξ baryons. The Lagrangian density for the free mesons involved is,

$$\begin{aligned} \mathcal{L}_M^{\text{free}} = & \frac{1}{2}(\partial_\mu \sigma \partial^\mu \sigma - m_\sigma^2 \sigma^2) + \frac{1}{2}(\partial_\mu \sigma^* \partial^\mu \sigma^* - m_{\sigma^*}^2 \sigma^{*2}) \\ & - \frac{1}{4}\omega_{\mu\nu}\omega^{\mu\nu} + \frac{1}{2}m_\omega^2\omega_\mu\omega^\mu - \frac{1}{4}\phi_{\mu\nu}\phi^{\mu\nu} + \frac{1}{2}m_\phi^2\phi_\mu\phi^\mu \\ & - \frac{1}{4}\rho_{\mu\nu}\rho^{\mu\nu} + \frac{1}{2}m_\rho^2\rho_\mu\rho^\mu. \end{aligned} \quad (3)$$

4 *A. Sulaksono*

The $\omega^{\mu\nu}$, $\phi^{\mu\nu}$ and $\rho^{\mu\nu}$ are field tensors corresponding to the ω , ϕ and ρ mesons field, and can be defined as $\omega^{\mu\nu} = \partial^\mu \omega^\nu - \partial^\nu \omega^\mu$, $\phi^{\mu\nu} = \partial^\mu \phi^\nu - \partial^\nu \phi^\mu$ and $\rho^{\mu\nu} = \partial^\mu \rho^\nu - \partial^\nu \rho^\mu$. The Lagrangian $\mathcal{L}_{BM}^{\text{lin}}$ describing interactions among baryons through mesons exchange is,

$$\begin{aligned} \mathcal{L}_{BM}^{\text{lin}} = & \sum_{B=N,\Lambda,\Sigma,\Xi} \bar{\Psi}_B [g_{\sigma B} \sigma + g_{\sigma^* B} \sigma^* - \gamma_\mu g_{\omega B} \omega^\mu \\ & - \frac{1}{2} \gamma_\mu g_{\rho B} \tau_B \cdot \rho^\mu - \gamma_\mu g_{\phi B} \phi^\mu] \Psi_B, \end{aligned} \quad (4)$$

where τ_B is the baryons isospin matrices. The Lagrangian describing mesons self interactions for σ , ω , and ρ mesons can be written as,

$$\begin{aligned} \mathcal{L}^{\text{nonlin}} = & -\frac{\kappa_3 g_{\sigma N} m_\sigma^2}{6m_N} \sigma^3 - \frac{\kappa_4 g_{\sigma N}^2 m_\sigma^2}{24m_N^2} \sigma^4 + \frac{\zeta_0 g_{\omega N}^2}{24} (\omega_\mu \omega^\mu)^2 \\ & + \frac{\eta_1 g_{\sigma N} m_\omega^2}{2m_N} \sigma \omega_\mu \omega^\mu + \frac{\eta_2 g_{\sigma N}^2 m_\omega^2}{4m_N^2} \sigma^2 \omega_\mu \omega^\mu \\ & + \frac{\eta_\rho g_{\sigma N} m_\rho^2}{2m_B} \sigma \rho_\mu \cdot \rho^\mu + \frac{\eta_{1\rho} g_{\sigma N}^2 m_\rho^2}{4m_N^2} \sigma^2 \rho_\mu \cdot \rho^\mu \\ & + \frac{\eta_{2\rho} g_{\omega N}^2 m_\rho^2}{4m_N^2} \omega_\mu \omega^\mu \rho_\mu \cdot \rho^\mu. \end{aligned} \quad (5)$$

While the free leptons Lagrangian density is,

$$\mathcal{L}_l^{\text{free}} = \sum_{l=e^-, \mu^-} \bar{\Psi}_l [i\gamma^\mu \partial_\mu - M_l] \Psi_l. \quad (6)$$

here Ψ_l is the leptons (electron and muon) field. The nucleons coupling constant and nonlinear parameters (BSP parameter set) are taken from Ref. 21. To determine the vector part of hyperons coupling constant $g_{\omega H}$ and $g_{\phi H}$, we consider conventional prescription based on SU(6) symmetry²⁴ i.e.,

$$\begin{aligned} \frac{1}{3} g_{\omega N} &= \frac{1}{2} g_{\omega \Lambda} = \frac{1}{2} g_{\omega \Sigma} = g_{\omega \Xi}, \\ g_{\rho N} &= \frac{1}{2} g_{\rho \Sigma} = g_{\rho \Xi}, \quad g_{\rho \Lambda} = 0, \\ 2g_{\phi \Lambda} &= 2g_{\phi \Sigma} = g_{\phi \Xi} = \frac{2\sqrt{2}}{3} g_{\omega N}, \quad g_{\phi N} = 0. \end{aligned} \quad (7)$$

For the given values of $g_{\omega H}$, the scalar hyperons coupling strengths $g_{\sigma H}$ are usually obtained from the potential depth of hyperons in the symmetric nuclear matter evaluated at the saturation density ρ_0 as,

$$U_H^{(N)}(\rho_0) = -g_{\sigma H} \sigma(\rho_0) + g_{\omega H} \omega(\rho_0), \quad (8)$$

where the values of experimentally potential depth $U_H^{(N)}$ at ρ_0 are²⁴

$$\begin{aligned} U_\Lambda^{(N)} &= -28 \text{ MeV}, \quad U_\Sigma^{(N)} = +30 \text{ MeV} \\ \text{and } U_\Xi^{(N)} &= -18 \text{ MeV}. \end{aligned} \quad (9)$$

The constituents composition in NS core is determined using standard conditions i.e., chemical potential balance, charge neutrality and baryon density conservation. The total energy density (ϵ) of NS core matter can be determined from the zero component of energy-momentum tensor (T^{00}) that is obtained from Eq. (1). The radial pressure p can be obtained from the thermodynamic relation as

$$p = \rho^2 \frac{d(\epsilon/\rho)}{d\rho}, \quad (10)$$

where ρ is baryon density.

3. Anisotropic Pressure in Spherical Symmetric Neutron Star

As it is mentioned in introduction, the possible sources of local pressure anisotropy in spherically symmetric gravitating bodies that consisting not only low but also high densities matters are well known since long times ago.⁴⁴ Note that local pressure anisotropy here means that the radial pressure p differs from the tangential pressure q . Many works after that up to now have been devoted to study this effect and to investigate the microscopic origin for each particular mechanism to generate pressure anisotropy in spherically symmetric gravitating bodies founded in the literature. Furthermore, reviews about many of the possible causes for the appearance of this effect and their main consequences are also already exist.^{41,52} However, it will be quite informative for the reader if the microscopic basis of anisotropy of the fluid pressure in spherically symmetric NS that produced from variety physical processes is briefly discussed.

(1) Electric field

In general, if matter is composed of several kind of particles with different masses and opposite electric charges like happens in compact stars, the presence of sharp discontinuity between surface of the star and vacuum should lead to a charge separation and generation of an electric field.⁵³ From conservative point of view, because the star is macroscopic object, the global charge neutrality must be fulfilled. Thus the positive charge from the baryons or quarks in a compact star should be balanced by negative charge of electrons. However, since electrons are light and only electromagnetically interacting, they will penetrate through the boundary and generate a local charge unbalanced around the star surface. The conditions leading to the generation of electric field at star boundary have been studied by the authors of Ref. 53. It is also reported that strange stars may be expected to carry huge electric fields on their surfaces^{54–56} thus it is quite wonder, if the electric field do not appear in NS surface. While it is known electrostatic interactions indeed are important for the description of neutron star crusts where atomic nuclei are embedded in dense electron gas.^{57,58} We need also to note that there is also a unconventional neutron star model proposed by using less stringent condition i.e., they used a local charge neutrality condition instead the global one so that the electric

field has been already explicitly taken into account in the corresponding model since the beginning.^{59–61} Furthermore, it is also claimed in Refs. 62–64 that for compact stars where the density is high and the relativistic effect is crucial, in principle, in the allowed net charge of a compact star; the star can take some more charge to be in equilibrium. We need also to note that in NS matter, Debye screening may be generated. It will ensure that electric fields are confined in microscopic length scale of 10–1000 fm. If we assume that the electric field is nonzero then the matter stress-energy tensor in the right hand side of Einstein equation with certain energy density and pressure will add with the terms from electromagnetic field, where for the case static and spherical symmetric stars, only the components of the Maxwell field F^{01} and F^{10} are survived. In this specific case the total radial and tangential pressures of the stars are not the same anymore i.e.,^{62–64}

$$q = p + \frac{1}{4\pi} \frac{Q^2}{r^4}, \quad (11)$$

where the total charge Q that produce electric field can be obtained from following relation

$$\frac{dQ}{dr} = 4\pi\rho_c \left[1 - \frac{2GM}{r} + \frac{GQ^2}{r^2} \right]^{-1/2} r^2. \quad (12)$$

Here ρ_c is charge density while M is total mass of the star. However, the actual form of ρ_c profile in each compact star case is indeed not certainly known. People usually use the parametrized form of ρ_c . For example, in the case electric field effect on strange star studied in Ref. 65, the authors used

$$\rho_c \equiv \frac{K}{4\pi r^2} [\delta(r - R^+) - \delta(r - R^-)], \quad (13)$$

to describe the charge distribution in that star. Here K is a parameter which identified the strength of the charge. However, in general the effect of electric field on standard picture of spherically symmetric NS properties are not too significant. For example, it is shown by the authors of Ref. 53 that under Newtonian gravitation approach, that the electrostatic and gravitational contributions become equal at minimum particle density $N_{min} \approx 6.26 \cdot 10^{36}$. This value corresponds to the mass M_{min} about 10^{13} gr, i.e. almost 20 order of magnitude smaller than the maximum mass of NS. (see the detail in Ref.53 and references therein). Note that the maximum allowed charge at the surface of NS with $M \approx M_\odot$ and radius R around 10 km, is $Q \lesssim 10^{20}$ C.⁶³ With this charge value, we can estimate that the expected observed neutron star anisotropy due to electric field is $q - p = \frac{1}{4\pi} \frac{Q^2}{R^4} \lesssim 5 \cdot 10^{-4} \text{ MeVfm}^{-3}$. It is much less compared to the center pressure of this corresponding NS, i.e., $p_c \sim 20 \text{ MeVfm}^{-3}$.

(2) Magnetic field

It is known from observations that pulsars have the typical surface magnetic field strength around 10^{12} – 10^{13} G⁶⁶ while the magnetars have surface magnetic

field strength in the range of 10^{14} - 10^{15} G.^{67,68} As also discussed in Ref. 67, the central magnetic field strength of the magnetars might be as high as 10^{18} - 10^{19} G. However, the origin of strong magnetic fields in compact stars is still not too clearly known up to now. The accepted large magnetic field generation mechanism in magnetars is based on amplification of a seed magnetic field owing to the rapidly rotating plasma of a protoneutron star. Nevertheless, this mechanism can not substantiate all of the features of the supernova remnants surrounding these objects (see Ref. 69 and references therein). Whatever the way to generate magnetic field in spherically symmetric compact stars, the presence of large magnetic field leads to the generation of pressure anisotropy, where if we neglected the small contribution from matter magnetization and assuming that the magnetic field in the radial direction, the total tangential pressure can be written as (see for example Ref. 70)

$$q = p + \frac{B^2}{4\pi}, \quad (14)$$

where B is the magnetic field in the corresponding star. Usually the magnetic profile of spherically symmetric NS is assumed to be density dependent and is parametrized as (see Ref. 70 and references therein)

$$B(\rho) \equiv B_s + B_0[1 - e^{-\alpha(\frac{\rho}{\rho_0})^\gamma}], \quad (15)$$

where α , γ are parameters, ρ_0 is saturation density, B_s and B_0 are surface and center magnetic fields of the star. However, we need to note, in previous studied that it is shown that the contribution of magnetic field in EOS of neutron star matter through magnetization is not too significant (see Ref. 70 and references therein). If we take $B \lesssim B_0 \approx 10^{18}$ G, the expected observed neutron star anisotropy due to magnetic field can be estimated as $q - p = \frac{B^2}{4\pi} \lesssim 2 \cdot 10^2 \text{ MeVfm}^{-3}$. We need to note that the strong magnetic field can affect also the surface electric field of strange stars.⁷¹ The presence of magnetic field in matter might be also lead to the polarization of matter. It was shown⁷² that the spin polarization induces a deformation of the Fermi spheres of nucleons with spins parallel and opposite to the polarization axes. This feature can be related to the structure of the one-pion exchange contribution to a realistic nucleon-nucleon interaction. The deformation is identified by angle dependent of Fermi momentum. This deformation will generate also additional pressure anisotropy (see detail discussion in Ref. 73).

(3) Beyond one fluid description

In conventional view, it is assumed that NS matter is an ideal one fluid composed by several kind of particles with different masses and opposite electric charges. However, if we consider NS matter as many fluids then the pressure anisotropy may appear in non trivial way. As an illustration, let see the simplest case. If we assume that the NS matter composed by 2 ideal fluids with different four velocity (u_μ and w_μ), fluid 1 composed by neutral particles and

8 *A. Sulaksono*

fluid 2 composed by charged particles.^{41,47,75} The total stress-energy tensor for this system becomes

$$\begin{aligned} T_{\mu\nu} &= (\epsilon_1 + p_1)u_\mu u_\nu + p_1 g_{\mu\nu} \\ &= (\epsilon_2 + p_2)w_\mu w_\nu + p_2 g_{\mu\nu}. \end{aligned} \quad (16)$$

Note, here we used metric sign $(-,+,+,+)$ instead $(+,-,-,-)$ which is used in Refs. 41,47,75. Therefore, the sign in some terms here is different to that presented in Refs. 41,47,74-75. Eq.(16) can be significantly simplified by casting it into standard form of anisotropic fluids. It can be done by using following transformation^{41,47,74,75}

$$\begin{aligned} u^{\mu*} &= u^\mu \cos\alpha + \left[\frac{\epsilon_2 + p_2}{\epsilon_1 + p_1} \right]^{1/2} w^\mu \sin\alpha \\ w^{\mu*} &= w^\mu \cos\alpha - \left[\frac{\epsilon_1 + p_1}{\epsilon_2 + p_2} \right]^{1/2} u^\mu \sin\alpha, \end{aligned} \quad (17)$$

where this transformation satisfies $T^{\mu\nu}(u, w) = T^{\mu\nu}(u^*, w^*)$. Explicitly it can be done by choosing $u^{\mu*}$ and $w^{\mu*}$ such that one is time-like and the other is space like so that $u^{\mu*}w_{\mu*}=0$, we can obtain the rotation angle in Eq. (17) as

$$\tan 2\alpha = 2 \frac{(\epsilon_2 + p_2)(\epsilon_1 + p_1)^{1/2}}{(\epsilon_2 + p_2) - (\epsilon_1 + p_1)} u^\mu w_\mu. \quad (18)$$

Followed by defining the quantities

$$\begin{aligned} v^\mu &= \frac{u^{\mu*}}{(-u^{\nu*}u_{\nu*})^{1/2}} & \kappa^\mu &= \frac{w^{\mu*}}{(w^{\nu*}w_{\nu*})^{1/2}} \\ \epsilon &= T^{\mu\nu}v_\mu v_\nu & \Psi &= T^{\mu\nu}\kappa_\mu \kappa_\nu \\ \Pi &= p_1 + p_2, \end{aligned} \quad (19)$$

respectively, then the $T^{\mu\nu}$ of two perfect fluids in Eq.(16) can be written as $T^{\mu\nu}$ of one fluid with anisotropy pressure as ^{41,47,74,75}

$$T_{\mu\nu} = \epsilon v_\mu v_\nu + \Psi \kappa_\mu \kappa_\nu + \Pi [g_{\mu\nu} + u_\mu u_\nu - \kappa_\mu \kappa_\nu]. \quad (20)$$

Note, To calculate this effect explicitly, beside the EOS of the matter, we need to know the magnitude of the scalar product of four velocity u_μ and w_μ . In principle, both velocities should be determined from other physics information where in some cases, it is unknown. For example, in Ref. 75 in the case of bosonic dark matter model, due to lack of such information, the authors used $u_\mu w^\mu$ as a parameter and studied the effect of the magnitude of this variable to the properties of bosonic dark matter. For providing rough estimation of the anisotropy effect from this mechanism, we may assume that only neutrons and protons dominate the contribution in energy density ϵ and pressure Π of NS. Now we denote the ϵ_1 and pressure p_1 as the energy density and pressure for proton fluid and ϵ_2 and pressure p_2 as the energy density and pressure for

neutron fluid and $u^\mu w_\mu \approx 1 + \frac{b}{2}$, where the b a number to identify the four-velocity difference between two fluids. By using Eqs. (6-7) in Ref. 75, it can be obtained that

$$\Psi - \Pi \approx \frac{b}{2} \frac{(\epsilon_1 + p_1)(\epsilon_1 + p_1)}{(\epsilon + \Pi)}, \quad (21)$$

if we approximate that $(\epsilon_1 + p_1) \approx Y_p(\epsilon + \Pi)$ and $(\epsilon_2 + p_2) \approx (\epsilon + \Pi)$, where Y_p is proton fraction, then $\Psi - \Pi \approx Y_p \frac{b}{2}(\epsilon + \Pi)$. It is known that the actual values of Y_p , ϵ and Π depend on the EOS model used. Parameter b also controls the significance of the effect. If the difference in four-velocity between two fluid is large the effect becomes larger and if it is small the effect is small. To estimate the number, lets for example say that the center density and its corresponding energy density for $M \approx M_\odot$ i.e., $\Pi_c \approx 20$ MeV with $\epsilon_c \approx 200$ MeV and $Y_p \sim 0.1$ as well as taking $b \sim 0.02$ than it leads to 10 % effect. Thus we may expect also a quite substantial effect may come from this mechanism.

(4) Other sources of anisotropy

Anisotropy in NS fluid pressure might be also yielded by the existence of a solid core or by the presence of superfluid and by pion condensation, as well as by different kind of phase transition (see Ref. 2 and references therein for more detail). Another source of pressure anisotropy may come also from the matter viscosity of NS (see Ref. 1 and references therein for more detail).

To this end, we need to emphasize here that the effect of local anisotropy in NS have been studied.^{2, 76-78} However, the discussion of NS local anisotropy by using more realistic and up to date NS matter EOS as well as by connecting this matter to the context of “hyperonization puzzle” is not yet done before and this becomes the focus of this work.

To accommodate the anisotropic fluid assumption, we start by taking the stress-energy tensor as:^{1, 2}

$$T_{\mu\nu} = \epsilon u_\mu u_\nu + p k_\mu k_\nu + q[g_{\mu\nu} + u_\mu u_\nu - k_\mu k_\nu]. \quad (22)$$

Here $g_{\mu\nu}$ is the space-time metric, u_μ is the fluid 4-velocity, ϵ is the total energy density, k_μ is the unit radial vector where $u^\mu k_\mu = 0$. At the center of symmetry, the anisotropic pressure must vanish since here k_μ is no longer defined. Note that $g_{\mu\nu} + u_\mu u_\nu - k_\mu k_\nu$ is the projection tensor onto the 2-surface orthogonal to k_μ and u_μ . Here, we use standard metric for spherically symmetric space time i.e.,

$$ds^2 = -e^{2\nu} dt^2 + e^{2\lambda} dr^2 + r^2(d\theta^2 + \sin^2\theta d\phi^2). \quad (23)$$

By inserting Eq. (22) into the Einstein field equations

$$R_{\mu\nu} - \frac{1}{2}g_{\mu\nu} = 8\pi G T_{\mu\nu}, \quad (24)$$

and followed by manipulating four equations from non-zero diagonal components of Eq. (24), we can obtain the Tolman-Oppenheimer-Volkoff (TOV) equations for

anisotropic star as follows

$$\frac{dp}{dr} = -G \frac{\epsilon M}{r^2} \left(1 + \frac{p}{\epsilon}\right) \left(1 + \frac{4\pi r^3 p}{M}\right) \left(1 - \frac{2GM}{r}\right)^{-1} - \frac{2\sigma}{r}, \quad (25)$$

while the mass and particles number profiles can be determined from

$$\begin{aligned} \frac{dM}{dr} &= 4\pi\epsilon r^2 \\ \frac{dA}{dr} &= 4\pi\rho r^2 \left(1 - \frac{2GM}{r}\right)^{-1/2}. \end{aligned} \quad (26)$$

Here the anisotropic pressure $\sigma = p - q$. It is obvious that if we set $p = q$ ($\sigma = 0$) in Eq. (25), we obtain the standard TOV equation for isotropic star. It is obvious that the last term in Eq. (25); σ , represents a kind of force which generated by anisotropy. This force can be directed outward or inward depending on the sign of σ . Therefore, we can have more massive configuration if σ is negative and less massive one if σ is positive. The strength and the distribution of the force depend on the magnitude of σ and its profile. Based on this mechanism, we can support larger masses and radii of neutron star even the EOS of matter is relative soft by adjusting σ . From above order of magnitude estimations, it can be seen also that electric field effect yields negligible effect on the magnitude of σ . The magnetic field may provide approximately $\sigma \lesssim -2 \cdot 10^2 \text{ MeVfm}^{-3}$. However, such a configuration of fluid and magnetic field that close to the upper bound of this estimation might lead to instability, and stable configurations likely have smaller σ . While if we used 2 fluids approach, σ depends on the value and sign of b , a parameter which shows the difference between the four-velocities of both fluids.

In principle, a realistic σ in Eq. (25) should be determined from the unified microscopic theory of matter. Unfortunately, as mentioned previously, the appearance of σ generate by interplay of many possible microscopic basis in such non trivial way. Then technically it is difficult to derive σ from one unified microscopic theory where it can capture effectively all source of anisotropy of matter. Furthermore, mostly the available microscopic models are developed in flat space-time because quantization process of many particles system in curve space-time is known very difficult. While the conventional transferred form of the stress-energy tensor to that for curve space-time, physically may not be too satisfactory (see discussions in Refs. 1-2, and the references therein). The following is a simple example to illustrate the later. Let us consider a star-like object that composing by scalar mesons. They interact each other by exchanging vector mesons.⁷⁹ If we consider both fields as classical fields, in flat space-time the field of both mesons are spatially homogeneous so that the pressure in stress-energy tensor in flat space-time is isotropic and the stress-energy tensor of the matter can be consider as 1 ideal fluid and as the consequence, in conventional view in curve space-time, stress-energy tensor of the system is also 1 ideal fluid and the structure can be obtained by solved the standard TOV equation for isotropic star.⁷⁹ However, in fact the spatially homogeneity of mesons fields in flat space-time does not always retain if it is transferred to curve

space-time. This can be seen obviously, if we directly calculate the stress-energy tensor of the matter in curve space-time (see example Ref. 80 for a particular case i.e., with the mass of vector meson is taken to be zero), we can obtain:

$$\begin{aligned}
T_0^0 &= -e^{-2\nu}[(\omega_\Phi + g_{V\phi}A)^2\Phi^2 + \frac{1}{2}m_V^2A^2 + \frac{1}{2}e^{-2\lambda}(\frac{dA}{dr})^2] \\
&\quad - [m_\Phi^2\Phi^2 + e^{-2\lambda}(\frac{d\Phi}{dr})^2] \\
T_r^r &= e^{-2\nu}[(\omega_\Phi + g_{V\phi}A)^2\Phi^2 + \frac{1}{2}m_V^2A^2 - \frac{1}{2}e^{-2\lambda}(\frac{dA}{dr})^2] \\
&\quad - [m_\Phi^2\Phi^2 - e^{-2\lambda}(\frac{d\Phi}{dr})^2] \\
T_\theta^\theta = T_\phi^\phi &= e^{-2\nu}[(\omega_\Phi + g_{V\phi}A)^2\Phi^2 + \frac{1}{2}m_V^2A^2 + \frac{1}{2}e^{-2\lambda}(\frac{dA}{dr})^2] \\
&\quad - [m_\Phi^2\Phi^2 + e^{-2\lambda}(\frac{d\Phi}{dr})^2], \tag{27}
\end{aligned}$$

where the vector and the scalar fields become inhomogeneous and obey following equations

$$\begin{aligned}
\frac{d^2A}{dr^2} + [\frac{2}{r} - (\lambda' + \nu')] \frac{dA}{dr} - e^{2\lambda}[m_V^2 \\
+ 2g_{V\phi}\Phi^2]A - 2g_{V\phi}\omega_\Phi\Phi^2e^{2\lambda} &= 0 \\
\frac{d^2\Phi}{dr^2} + [\nu' - \lambda' + \frac{2}{r}] \frac{d\Phi}{dr} \\
+ e^{2\lambda}[e^{-2\nu}((\omega_\Phi + g_{V\phi}A)^2 - m_\Phi^2)]\Phi &= 0. \tag{28}
\end{aligned}$$

It is obvious from Eq. (27) that the radial pressure p (T_r^r) and the tangential pressure q (T_θ^θ) of this system are not the same anymore due to the presence of nonzero value of $\frac{dA}{dr}$ and $\frac{d\Phi}{dr}$. How large such effect, is only be known by solving Eqs. (27-28) explicitly. But this is already the outside of the scope of this work. Second example of this situation can be seen if we consider a star matter that composed by ideal relativistic free Fermi gas. It is well known, if we quantized in flat space-time, and transferred its energy-momentum tensor to curve space-time by conventional manner, then we obtain the pressures of this matter is isotropic. However, the author of Ref. 81 demonstrated that if we directly solve the Dirac equation of N free Fermion system in curve space-time, then it is obtained that the pressures of matter becomes anisotropic.

Therefore, based on these twofold difficulties, the expression of q should be modeled. The following conditions are general physical requirements for physically meaningful anisotropic fluid spheres^{41, 82}

- (1) the energy ϵ and p should be positive inside the star;
- (2) the gradients $\frac{d\epsilon}{dr}$, $\frac{dp}{dr}$, and $\frac{dq}{dr}$ should be negative;
- (3) inside the static configuration the speed of sound should be less than the speed of light, i.e., $0 \leq \frac{dp}{d\epsilon} \leq 1$ and $0 \leq \frac{dq}{d\epsilon} \leq 1$;

12 *A. Sulaksono*

- (4) energy momentum tensor has to be obey the conditions $\epsilon \geq p + 2q$ and $\epsilon + p + 2q \geq 0$;
- (5) the interior metric should be joined continuously with exterior Schwarzschild metric;
- (6) the p must vanish but q may not vanish at boundary $r=R$ of the sphere, but both should be equal at the center of the matter configuration.

Therefore, in the modeling of q must not deviate from these general requirements. In this work, we do not propose a new model but only select two models of q which are quite often studied in communities.^{1, 2, 45, 46, 83–85} The first model is obtained by heuristic procedure which allows one to obtain solutions for anisotropic matter from known solutions for isotropic matter.^{1, 46} See more detail about the procedure used to get this model (HB) of q in Ref. 46. In HB model, q depends on p and $\frac{dp}{dr}$. The second model (DY) is taken from Refs. 2,45 where q is quasi-local EOS. In DY model, q depends directly on p and local compactness $\frac{2GM}{r}$ as a quasi-local variable. See more detail about how to construct quasi-local EOS, q and its thermodynamics in Refs. 45,84–85. The explicit q form of both models, respectively are

$$q = p[1 - \Lambda(\frac{2MG}{r})], \quad (29)$$

$$q = p + \frac{r}{2} \frac{(1-h)}{h} (\frac{dp}{dr}), \quad (30)$$

where Λ and h are anisotropic parameters. For isotropic stars, parameters Λ and h should be equal to 0 and 1, respectively. Thus, the deviation from its reference value of $\Lambda=0$ or $h=1$ shows the degree of an anisotropy. We need also to note that Refs. 1-2 used polytopes EOS to describe the matter. They also investigate the effects of the variation of both parameters in the range of $-2 \leq \Lambda \leq 2^2$ and $0.5 \leq h \leq 1.5$ ¹ using this EOS. The authors of Ref. 1 found that we can have more massive star if we use $\Lambda < 0$ while the authors of Ref.¹ found that more massive star can be obtained if we use positive h and $h < 1$. In addition, in the case of DY model, for large magnitude of Λ and large masses, NS solution exists for which the energy density ϵ is not a monotonic function of the radial coordinate but is maximum. While these solutions are dynamically stable,^{2,45} Ref. 1 shows for the HB model that the stability of this model increases with the decrease of h .

Here gravitation mass is defined as $M_G=M(R)$ and $A(R)$ is multiplied by atomic unit. 931.50 MeV defines the baryonic mass M_B where R is the star radius. Note, general relativity predicts a redshift for photons leaving the surface of the star with strong gravitational field. The gravitational redshift of a non-rotating NS is indicated by

$$Z = (1 - \frac{2GM}{r})^{-1/2} - 1. \quad (31)$$

By solving Eq. (25), numerically, we can study the effects of anisotropic pressure on the NS gravitational mass-radius relation, NS minimum mass and Z through Eq. (31).

4. Results and Discussion

In this section, we discuss the effects of anisotropic pressure on some NS properties using one of the parameters in the ERMF model. We adopt the BSP parameter set because this parameter set provides good descriptions of the global properties of finite nuclei, and its prediction of nuclear matter properties is quite compatible to the prediction from the heavy ion data. For meson-hyperon couplings, we use conventional SU(6) symmetry and the experimental values of nuclear matter potential depths hyperons in the nuclear matter at ρ_0 .²⁴

In the upper panel of Fig. 1, we present the NS gravitational mass-radius relation for the case of isotropic pressure (I-P) with and without hyperons (no hyperon) as well as the cases of anisotropic pressure (AI-P) using DY and HB models, respectively. The mass of PSR J0348+0432 is taken from Ref. 5 while PSR J1614-2230 is from Ref. 4. The dot and circle markers indicate respectively NS M_{\max} and canonical radius (radius where $M_G=1.4 M_\odot$). It can be observed that if we assume the NS matter pressure is isotropic (I-P case), the maximum mass decreases from $M_G=2.02 M_\odot$ to $M_G=1.74 M_\odot$ if hyperons are allowed to appear in the NS core. The value $M_G=1.74 M_\odot$ is obviously outside the mass range of PSR J0348+0432 and PSR J1614-2230. However, if we allow that the pressure of NS matter to be anisotropic (AI-P case) we can obtain maximum mass greater than the masses of PSR J0348+0432 and PSR J1614-2230 for $\Lambda \leq -1.15$ ($M_G=2.08 M_\odot$) for DY² and $h \leq 0.8$ ($M_G=2.09 M_\odot$) for the HB¹ models used. These results can be achieved without adjusting the hyperons coupling constant, introducing hypothetical particle like WILB or modifying the nonlinear terms in the strange meson sector.^{29–33} Furthermore, by assuming that NS matter may have anisotropic pressure, the NS maximum mass limit higher than $2.1 M_\odot$ cannot rule out the presence of exotica in the form of hyperons, boson condensations or quark matter inside the NS core. For I-P case, the canonical radius with hyperons is $R_{1.4}=12.57$ km, and $R_{1.4}=12.61$ km without hyperons. These values are almost the same as there are only very small amount of hyperons already present in isotropic NS with $M_G = 1.4M_\odot$. For AI-P case, the $R_{1.4}$ is relatively higher than that in the I-P cases. DY model predicts $R_{1.4}=13.00$ km for $\Lambda = -1.15$ while HB model predicts $R_{1.4}=13.69$ km for $h = 0.8$. If we compare our result with the radius constraint from X-ray bursts, it can be seen that the radii predicted by all models considered here are greater than the radius constraint as obtained by Steiner *et. al*¹⁷ but smaller than that of Sulaimanov *et. al*.¹⁹ If we compare our result with the radius constraint from quiescent low mass X-ray binaries, the radii result predicted by all models are greater than the radii constraint as in Guillot *et. al*¹³ but are barely compatible to the result obtained by Lattimer and Steiner.¹⁴ However, these results are compatible with the lower limit of radius of pulsar J0437-4715 i.e., $R > 11.1$ km within 3σ error.¹² Therefore, more accurate radius measurement from other possible sources is needed to test the reliability of the anisotropic models.

In the lower panel in Fig. 1, we present gravitational mass versus baryonic mass

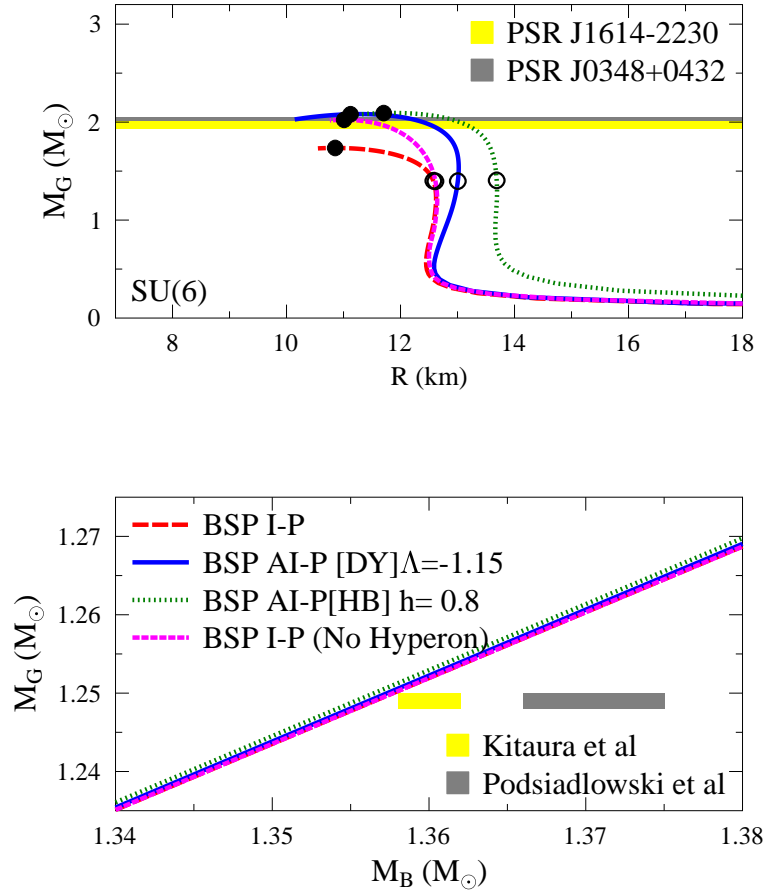


Fig. 1. Upper panel: The plots for NS gravitational mass-radius relation for the case of isotropic pressure (I-P) with and without hyperons as well as the cases of anisotropic pressure (AI-P). The mass of PSR J0348+0432 is taken from Ref.⁵ while the mass of PSR J1614-2230 is from Ref.⁴ Lower panel: The plots for the corresponding gravitational mass versus baryonic mass for small NS. The shaded boxes are simulation results by Kitaura *et. al*⁸⁷ and Podsiadlowski *et. al*.⁸⁶ DY indicates the result obtained by using σ of Ref.² and HB is obtained by using σ of Ref.¹ The dot and circle markers indicate NS M_{\max} and canonical radius ($M_B=1.4 M_\odot$) respectively. Note that for all NS with hyperons inside its core, the hyperon-meson coupling strength is determined by using SU(6) symmetry.

for NS with $M_G < 1.27 M_\odot$. It is obvious in this region that hyperons yield negligible effect while the effect of anisotropic pressure is apparently insignificant. We note, the double pulsar J0737-3039 and its interpretation poses a constraint for this low mass region.⁸⁶ The gravitational mass of pulsar B is measured very precisely while

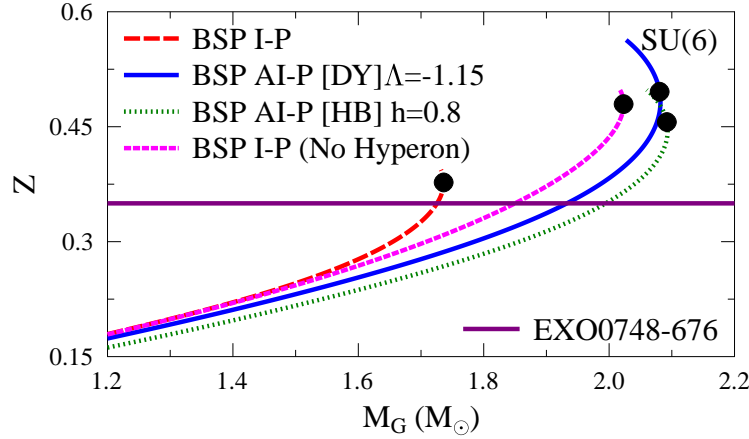


Fig. 2. The gravitational redshift Z of NS as a function of NS gravitational mass for the cases of isotropic pressure (I-P) with and without hyperons as well as the cases of anisotropic pressure (AI-P). The horizontal line is Z for low mass X-ray binary EXO0748-676 NS (Ref.⁸⁸). The dot marker indicates Z at M_{max} . Note that for all NS with hyperons inside its core, the hyperon-meson coupling strength is determined by using SU(6) symmetry.

the baryonic mass depends on the mode of its creation, which can be modeled. The shaded boxes are simulation results in the form of gravitational mass as a function of baryonic mass obtained by Kitaura *et. al.*⁸⁷ and Podsiadlowski *et. al.*⁸⁶ It can be observed that our results by using BSP parameter set are barely compatible to the result of simulation by Kitaura *et. al.*. We also note that our result is also relatively close to the calculation result by using the quark-meson coupling model as obtained by Whittbury *et. al.*⁴⁰

In Fig. 2, we present the redshift Z as the function of NS gravitational mass for I-P and AI-P cases by using the HB and DY models for the EOS of NS core with and without hyperons. The result is also compared to the observational constraint from EXO0748-676.⁸⁸ This constraint implies that the acceptable EOS should have maximum Z above 0.33.²³ It can be seen that for all cases, the results are consistent with $Z = 0.35$ for the mass greater than $1.7 M_{\odot}$. These results are quite consistent with the expected higher masses of accreting stars in X-ray binaries. It can also be observed that the value of Z at M_{max} in AI-P cases is higher than that in I-P cases with hyperons. However, this result is quite similar to the one in I-P cases without hyperons. This is due to the stiffening of EOS for the AI-P case. The fact that the radius of NS at M_{max} predicted by HB with $h = 0.8$ ($R[M_{\text{max}}] = 11.70$ km) is slightly greater than that predicted by DY with $\Lambda = -1.15$ ($R[M_{\text{max}}] = 11.12$ km) is the reason why the Z at M_{max} predicted by DY model is higher than the Z in

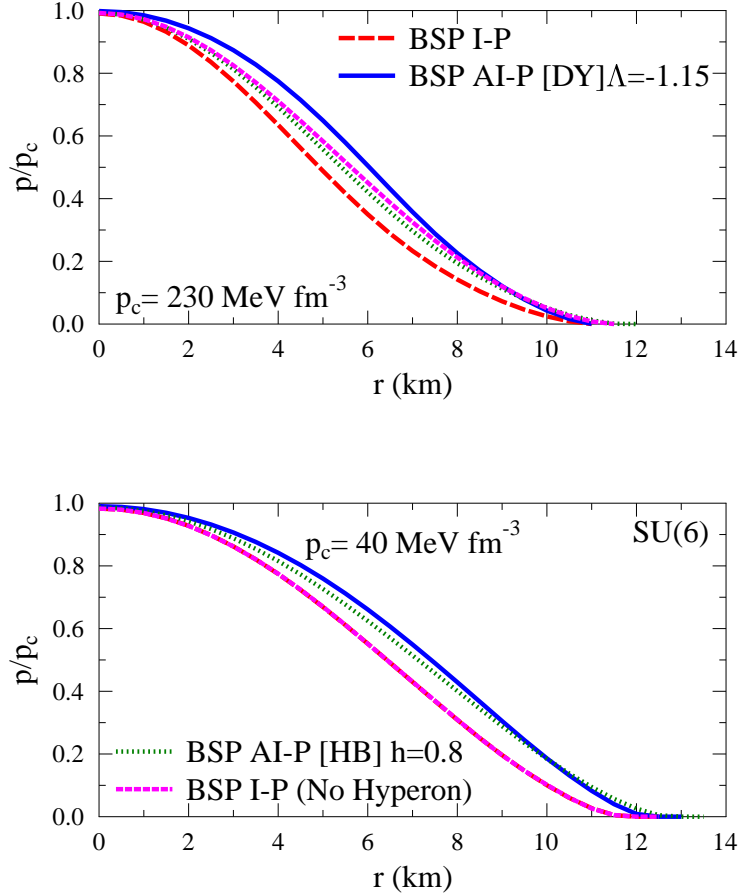


Fig. 3. The ratio of the radial pressure p to its value at the center p_c as a function of radial coordinate r for an NS with $p_c = 40 \text{ MeV fm}^{-3}$ (lower panel) and for an NS with $p_c = 230 \text{ MeV fm}^{-3}$ (upper panel) in the case of isotropic pressure (I-P) with and without hyperons as well as in the case of anisotropic pressure (AI-P). Note that for all NS with hyperons inside its core, the hyperon-meson coupling strength is determined by using SU(6) symmetry.

the HB model.

To investigate further, in Figs. 3 and 4 we plot the ratio of the radial pressure p to its value at the center p_c and the ratio of the energy density ϵ to its value at the center ϵ_c as a function of radial coordinate r . The results plotted in the lower and upper panels correspond to the central pressure $p_c = 40$ and 230 MeV fm^{-3} , respectively. For $p_c = 40 \text{ MeV fm}^{-3}$, BSP AI-P [DY] has $M_G = 1.47 M_\odot$, BSP AI-P [HB] has $M_G = 1.55 M_\odot$, BSP I-P with and without hyperons yield identical

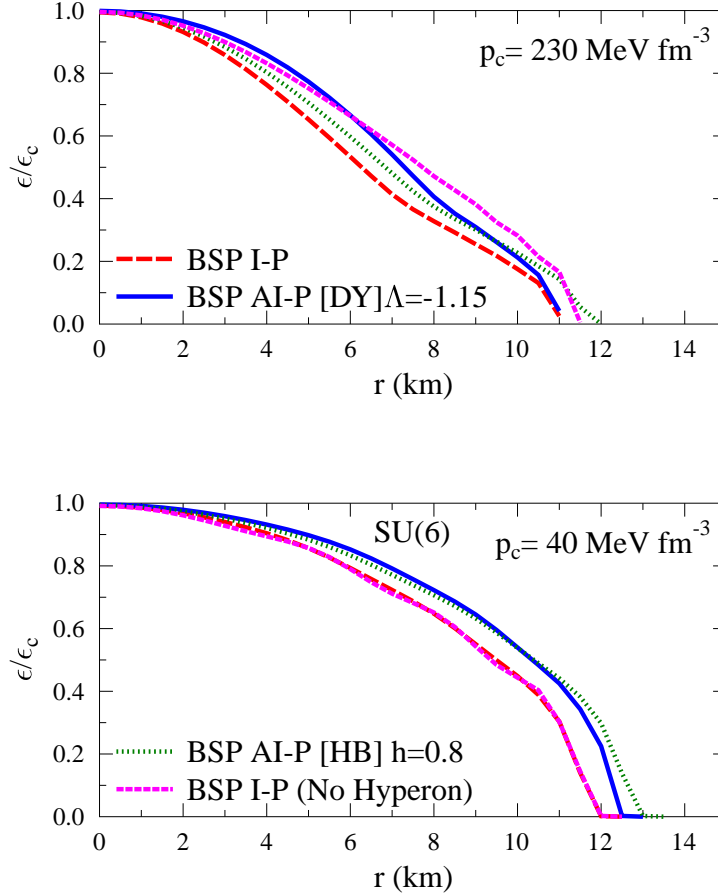


Fig. 4. Similar to Fig. 3 but for the ratio of energy density to the value in center as a function of radial coordinate r for an NS with $p_c = 40 \text{ MeV fm}^{-3}$ (lower panel) and for an NS with $p_c = 230 \text{ MeV fm}^{-3}$ (upper panel).

mass i.e., $M_G = 1.19 M_\odot$, because for these cases hyperons have not yet appeared in NS and the effects on the pressure profile are only due to the anisotropy. For $p_c = 230 \text{ MeV fm}^{-3}$, BSP AI-P [DY] yields $M_G = 2.1 M_\odot$, BSP AI-P [HB] yields $M_G = 2.1 M_\odot$, and BSP I-P yields $M_G = 1.7 M_\odot$ but BSP I-P (no-Hyperons) has $M_G = 1.9 M_\odot$. In this case, we can observe the effects of the interplay of hyperons and anisotropy roles.

The absence of hyperons slowly decreases p and ϵ with increase in the distance from the center of a NS. The role of anisotropic pressure is the same as that of the case with no hyperons, i.e., p and ϵ decreases slowly with increase in the distance

from the center of a NS. But at low p_c or ϵ_c values, the anisotropic pressure still yields pronounced impact. However, effect of AI-P in slowing down the rate of decreasing p and ϵ due to application of different anisotropy models appears more significant at relatively high radial p_c or ϵ_c values. The latter can be understood by observing the plots of anisotropic pressure σ of NS with hyperons from the HB and DY models as a function of radial coordinate r and mass distribution M which are shown in Figs. 5 and 6. It can be observed that unlike the HB model with almost constant absolute value of maximum anisotropic pressure σ , the prediction using the DY model is rather sensitive to the value of p_c . DY model predicts greater σ for higher p_c . For $p_c = 40 \text{ MeV fm}^{-3}$, the DY model predicts absolute value of maximum $\sigma \sim 0.1 \text{ MeV fm}^{-3}$ at $M \sim 0.4 M_\odot$ and $r \sim 7 \text{ km}$ while the HB model predicts the same absolute value of maximum σ at $M \sim 0.8 M_\odot$ and $r \sim 10 \text{ km}$. For $p_c = 230 \text{ MeV fm}^{-3}$ on the other hand, the DY model predicts absolute value of maximum $\sigma \sim 0.2 \text{ MeV fm}^{-3}$ at $M \sim 0.6 M_\odot$ and $r \sim 6 \text{ km}$ while the BD model predicts the absolute value of maximum $\sigma \sim 0.1 \text{ MeV fm}^{-3}$ at $M \sim 0.7 M_\odot$ and $r \sim 6 \text{ km}$. To this end, it is clear that if we use the EOS of NS core without hyperons as a reference, the presence of hyperons in NS core suppresses the EOS stiffness by decreasing p or ϵ but by allowing the NS pressure anisotropic, the stiffness of the EOS is pulled back to relatively higher p or ϵ so that the $M_{\text{max}} \geq 2.1 M_\odot$ can be reached. However, some details such as the radius prediction still depend significantly on the model used to describe the anisotropic pressure. Therefore, beside the existence of more accurate NS observable data like mass, radius etc, it seems that systematic reassessment of the consistency of the anisotropic pressure models offer in the literature with all possible physical requirements for anisotropic star including the star stability using “realistic matter EOS” are important to select the most physically acceptable model. However, this is already outside the scope of this work. We leave it as our next project.

5. Conclusion

We have studied the effect of anisotropic pressure on the gravitational mass, baryonic mass, radius and the redshift of static NS with the presence of hyperons in NS core. The BSP parameter set of the ERMF model²¹ and standard SU(6) symmetry as well as the experimental value of nuclear matter potential depths are used to determine the hyperon-meson coupling constants.²⁴ To describe the anisotropic pressure we adopt two known models in the literature, namely DY² and HB¹ models. The effect of anisotropic pressure on NS matter is mainly to increased stiffness of the NS EOS. This effect can compensate the softening of the NS EOS due to the presence of hyperons. Without further adjusting the hyperons coupling constant, introducing hypothetical particle like WILB or modifying the nonlinear terms in strange meson sector,^{29–33} we can easily obtain larger M_G than the masses of PSR J0348+0432 and PSR J1614-2230 if $\Lambda \leq -1.15$ for DY² and $h \leq 0.8$ for HB¹ models are used. In anisotropic NS, the maximum mass limit higher than $2.1 M_\odot$

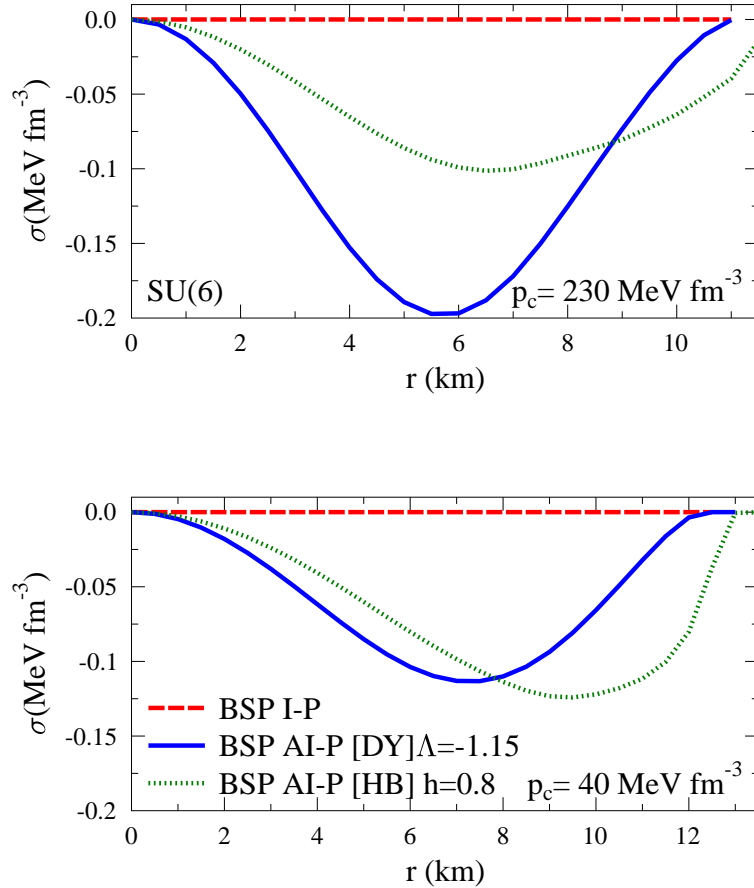


Fig. 5. Similar to Fig. 3 but for the anisotropic pressure σ of NS with hyperons inside its core as a function of radial coordinate r for an NS with $p_c = 40 \text{ MeV fm}^{-3}$ (lower panel) and for an NS with $p_c = 230 \text{ MeV fm}^{-3}$ (upper panel).

cannot rule out the presence of exotica in the form of hyperons, boson condensations or quark matter inside the NS core. We have found relatively large canonical radius. DY model predicts $R_{1.4}=13.00$ km for $\Lambda = -1.15$ and HB model predicts $R_{1.4}=13.69$ km for $h = 0.8$. We also found that the relation between gravitation mass and baryon NS mass remain practically unaffected for $M_G < 1.27 M_\odot$ due to the anisotropic pressure. Furthermore, the anisotropic pressure can increase the value of Z at maximum mass. We also show that the minimum mass, radius and the redshift predictions of anisotropic NS are quite compatible with the recent observational constraints.

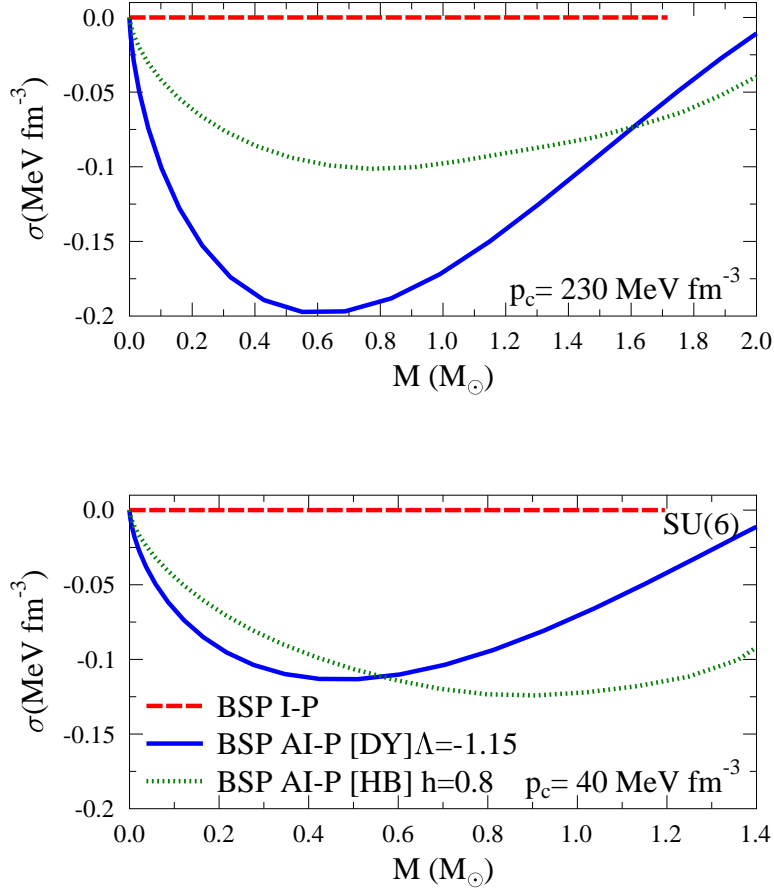


Fig. 6. Similar to Fig. 3 but for the anisotropic pressure σ of NS with hyperons inside its core as a function of its mass distribution $M(r)$ for an NS with $p_c = 40 \text{ MeV fm}^{-3}$ (lower panel) and for an NS with $p_c = 230 \text{ MeV fm}^{-3}$ (upper panel).

Acknowledgments

A. S. acknowledges the support given by Universitas Indonesia through Hibah Klaster Riset 2014 (No:1709/H2.R12/HKP.05.00/2014). A. S. also want to express many thanks to Prof. B. K. Agrawal for checking thoroughly the English of this paper.

References

1. L. Herrera and W. Barreto, *Phys. Rev. D* **88**, (2013) 084022.
2. D. D. Doneva and S. S. Yazadjiev, *Phys. Rev. D* **85**, (2012) 124023.

3. B. Kiziltan, A. Kottas, M. D. Yoreo, and S. E. Thorsett, *Astrophys. J* **778**, (2013) 66.
4. P. B. Demorest, T. Pennucci, S. M. Ransom, M. S. E. Roberts, and J. W. T. Hessels, *Nature* **467**, (2010) 1081.
5. J. Antoniadis, *et al*, *Science* **340**, (2013) 6131.
6. M. H. van Kerkwijk, R. P. Brenton, and S. R. Kulkarni, *Astrophys. J* **728**, (2011) 95.
7. R. W. Romani, *et al*, *Astrophys. J. Lett* **760**, (2012) L36.
8. M. C. Miller, arXiv:1312.0029.
9. J. M. Lattimer, *Annu. Rev. Nuc. Part. Sci* **62**, (2012) 485.
10. N. Chamel, P. Haensel, J. L. Zdunik, and A. F. Fantina, *Int. J. Mod. Phys. E* **22**, (2013) 1330018.
11. J. M. Lattimer and M. Prakash, arXiv:1012.3208.
12. S. Bogdanov, *Astrophys. J* **762**, (2013) 96.
13. S. Guillot, M. Servillat, N. A. Webb, and R. E. Rutledge, *Astrophys. J* **772**, (2013) 7.
14. J. M. Lattimer and A. W. Steiner, arXiv:1305.3242.
15. D. A. Leahy, S. M. Morsink, and Y. Chou, *Astrophys. J* **742**, (2011) 17.
16. F. Özel, G. Baym, and T. Güver, *Phys. Rev. D* **82**, (2010) 101301.
17. A. W. Steiner, J. M. Lattimer, and E. F. Brown, *Astrophys. J* **722**, (2010) 33.
18. A. W. Steiner, J. M. Lattimer, and E. F. Brown, *Astrophys. J. Lett* **765**, (2013) L5.
19. V. Sulaimanov, J. Poutanen, M. Revnivtsev, and K. Werner, *Astrophys. J* **742**, (2011) 122.
20. F. J. Fattoyev, C. J. Horowitz, J. Piekarewicz, and G. Shen, *Phys. Rev. C* **82**, (2010) 055803.
21. B. K. Agrawal, A. Sulaksono, and P.-G. Reinhard, *Nucl. Phys. A* **882**, (2012) 1.
22. J. L. Zdunik, and P. Haensel, *Astron. Astrophys* **551**, (2013) A61.
23. B. D. Lackey, M. Nayyar, and B. J. Owen, *Phys. Rev. D* **73**, (2006) 024021.
24. J. Schaffner-Bielich, and A. Gal, *Phys. Rev. C* **62**, (2000) 034311.
25. G. F. Burgio, H.-J. Schulze, and A. Li, *Phys. Rev. C* **83**, (2011) 025804.
26. H.-J. Schulze and T. Rijken, *Phys. Rev. C* **84**, (2011) 035801.
27. I. Vidãna, D. Logoteta, C. Providência, A. Polls, and I. Bombaci, *Europhys. Lett* **94**, (2011) 11002.
28. D. Lonardoni, A. Lovato, S. Gandolfi and F. Pederiva, arXiv:1407.4448.
29. I. Bednarek, P. Haensel, J. L. Zdunik, M. Bejger, and R. Mañka, *Astron. Astrophys* **543**, (2012) A157.
30. A. Sulaksono and B. K. Agrawal, *Nucl. Phys. A* **895**, (2012) 44.
31. W.-Z. Jiang, B.-A. Li, and L.-W. Chen, *Astrophys. J* **756**, (2012) 56.
32. S. Weissenborn, D. Chatterjee, and J. Schaffner-Bielich, *Phys. Rev. C* **85**, (2012) 065802.
33. A. Sulaksono, Marliana, and Kasmudin, *Mod. Phys. Lett. A* **26**, (2011) 367.
34. J. R. Stone, P. A. M. Guichon, and A. W. Thomas, arXiv:1012.2919.
35. C.-Y. Ryu, C.H. Hyun, and C.-H. Lee, *Phys. Rev. C* **84**, (2011) 035809.
36. R. Mallick, arXiv:1207.4872.
37. C. H. Lenzi and G. Lugones, *Astrophys. J* **759**, (2012) 57.
38. G. Colucci and A. Sedrakian, *Phys. Rev. C* **87**, (2013) 055806.
39. T. Miyatsu, S. Yamamuro, and K. Nakazaki, *Astrophys. J* **777**, (2013) 4.
40. D. L. Whittenbury, J. D. Carrol, A. W. Thomas, K. T. Tsushima, and J. D. Stone, arXiv:1307.4166.
41. L. Herrera and N. O. Santos, *Phys. Rep.* **286**, (1997) 53.

42. V. Canuto, *Annu. Rev. Astron. Astrophys* **12**, (1974) 167.
43. I. Lovas, L. Molnar, K. Sailer, and W. Greiner, *Phys. Rev. C* **45**, (1992) 1693.
44. R. L. Bowers and E. P. T. Liang, *Astrophys. J* **88**, (1974) 657.
45. D. Horvat, S. Ilicic, and A. Marunovic, *Classical Quantum Gravity* **28**, (2011) 025009.
46. M. Cosenza, L. Herrera, M. Esculpi, and L. Witten, *J. Math. Phys. (N.Y.)* **22**, (1981) 118.
47. T. Harko and F. S. N. Lobo, *Phys. Rev. D* **83**, (2011) 124051.
48. P. H. Nguyen and J. F. Pedraza, *Phys. Rev. D* **88**, (2013) 064020.
49. J. P. Mimoso, M. Le Delliou, and F. C. Mena, *Phys. Rev. D* **88**, (2013) 043501.
50. R. Furnstahl, B. D. Serot, and H-B. Tang, *Nucl. Phys. A* **598**, (1996) 539.
51. R. Furnstahl, B. D. Serot, and H-B. Tang, *Nucl. Phys. A* **615**, (1997) 441.
52. B. V. Ivanov, *Int. J. Theor. Phys* **49**, (2010) 1236.
53. I. N. Mishustin, C. Ebel and W. Greiner, *J. Phys. G* **37**, (2010) 075201.
54. C. Alcock, E. Farhi, and V. Olinto, *Astrophys. J* **310**, (1986) 261.
55. Ch. Kettner, F. Weber, M. K. Weigel, and N. K. Glendenning, *Phys. Rev. D* **51**, (1995) 1440.
56. V. V. Usov, *Phys. Rev. D* **70**, (2004) 067301.
57. G. Baym, H. A. Bethe, and C. J. Pethick, *Nucl. Phys. A* **175**, (1971) 225.
58. T. J. Burvenich, I. N. Mishustin and W. Greiner, *Phys. Rev. C* **76**, (2007) 034310.
59. R. Belvedere, D. Pugliese, J. A. Rueda, R. Ruffini and S.-S. Xue, *Nucl. Phys. A* **883**, (2012) 1.
60. R. Belvedere, K. Boshkayev, J. A. Rueda, and R. Ruffini, *Nucl. Phys. A* **921**, (2014) 33.
61. J. A. Rueda, R. Ruffini, Y.-B. Wu, and S.-S. Xue, *Phys. Rev. C* **89**, (2014) 035804.
62. J. D. Bekenstein, *Phys. Rev. D* **4**, (1971) 2185.
63. S. Ray, A. L. Espindola, M. Malheiro, J. P. S. Lemos and V. T. Zanchin, *Phys. Rev. D* **68**, (2003) 084004.
64. J. D. V. Arbañil, J. P. S. Lemos and V. T. Zanchin, *Phys. Rev. D* **88**, (2013) 084023.
65. R. Picanco Negreiros, I. N. Mishustin, S. Schramm and F. Weber, *Phys. Rev. D* **82**, (2010) 103010.
66. J. H. Taylor, R. N. Manchester, and A. G. Lyne, *Astrophys. J* **88**, (1993) 529.
67. C. Thompson and R. C. Duncan, *Astrophys. J* **392**, (1992) L9.
68. C. Thompson and R. C. Duncan, *Astrophys. J* **473**, (1996) 322.
69. E. J. Ferrer, V. de la Incera, J. P. Keith, I. Portillo and P. L. Springsteen, *Phys. Rev. C* **82**, (2010) 065802.
70. R. Mallick and S. Schramm, *Phys. Rev. C* **89**, (2014) 045805.
71. X. P. Zheng and Y. W. Yu, *Astron. Astrophys* **445**, (2006) 627.
72. T. Frick, H. Muther and A. Sedrakian, *Phys. Rev. C* **65**, (2002) 061303.
73. E. S. Corchero, *Classical Quantum Gravity* **15**, (1998) 3645.
74. S. S. Bayin, *Phys. Rev. D* **26**, (1982) 1262.
75. P. S. Letelier and P. S. C. Alencar, *Phys. Rev. D* **34**, (1986) 343.
76. H. Heintzmann and W. Hillebrandt, *Astron. Astrophys* **38**, (1975) 51.
77. H. Heintzmann and K. O. Steinmetz, *Astron. Astrophys* **53**, (1976) 283.
78. M. K. Mak and T. Harko, *Proc. R. Soc. A* **459**, (2003) 393.
79. P. Agnihotri, J. Schaffner-Bielich, and I. N. Mishustin, *Phys. Rev. D* **79**, (2009) 084033.
80. D. Pugliese, H. Quevedo, Jorge A. RuedaH, and R. Ruffini, *Phys. Rev. D* **88**, (2013) 024053.
81. E. S. Corchero, *Astrophys. Space Sci* **275**, (2001) 259.
82. M. K. Mak and T. Harko, *Ann. Phys. (Leipzig)* **11**, (2002) 3.

- 83. L. Herrera and W. Barreto, *Phys. Rev. D* **87**, (2013) 087303.
- 84. A. De Benedictis, D. Horvat, S. Ilijic, S. Kloster, and K. S. Visawanathan, *Classical Quantum Gravity* **23**, (2006) 2303.
- 85. C. Cattoen, T. Faber, and M. Visser, *Classical Quantum Gravity* **22**, (2005) 4189.
- 86. Ph. Podsiadlowski, *et al*, *Mon. Not. R. Astron. Soc* **361**, (2005) 1243.
- 87. F. S. Kitaura, H.-Th. Janka, and W. Hillebrant, *Astron. Astrophys* **450**, (2006) 345.
- 88. J. Cottam, F. Pearce, and M. Mendez, *Nature* **420**, (2002) 51.